Upper Ocean Variability of Mesoscale Structures in the Gulf of Mexico with Significant Larvae Recruitment Effects during Spring Months

David Lindo, Francis Bringas, Gustavo Goni and Barbara Muhling

1. Introduction

The Gulf of Mexico (GOM) is characterized by a complex and highly variable circulation, in time and space. This variability is the result of process interactions at basin, sub-basin and local scales, and results in dynamically significant modifications of the sub-basin scale variability. Variability of ocean properties is expected to have a direct effect on ecosystems in the Gulf of Mexico. This region is very diverse biologically, being the site for spawning and habitat of several pelagic and benthic species. Fisheries predictive tools can be enhanced by incorporating new observing capabilities, which resolve physical processes at a wide range of scales.

The mesoscale circulation in the GOM is dominated by three main features: the Loop Current (LC), the rings shed by the LC, and a quasi-permanent gyre in the south (Figure 1). When investigating larval fish distributions, these ocean features need to be considered (Bakun, 2006). The LC extends northward into the GOM from the Yucatan Channel. The current forms an intense anticyclonic flow, which can extend as far north as 29.1°N and can come within close proximity to the Mississippi River delta or the Florida Panhandle coast (Molinari and Mayer, 1982). Although the LC intrusion may tend to form more frequently in the spring, it may occur in any season and with periods varying from 6 to 17 months (Molinari, 1980) with an average period of 10-11 months (Maul, 1993).

The LC returns to its direct configuration by slowly pinching off its northern extension to form large, warm-core rings that then propagate westward at speeds of 2-5 km/day, and have lifetimes of days to approximately a year (Elliott, 1982; Forristal *et al.*, 1992; Shay *et al.*, 1998). These large anticyclonic rings shed by the LC with radii of approximately 150 km, swirl speeds of 1.8-2 m/s, and around 800 m depth (Oey *et al.*, 2005) are generated aperiodically, with an average shedding time of 9.5 months and a range of 3 to 21 months between consecutive sheddings (Sturges A., and Leben, 2000). The separation process can take several days to a few weeks, and often, after a ring has separated, it reattaches to the LC (Sturges et al, 1993). The separations of these large anticyclonic rings are the most energetic events in the circulation of the GOM. The bathymetry has a strong influence on the circulation, since the entrances of the Gulf are constricted by two wide and shallow continental shelves, the Campeche Bank and the West Florida Shelf.

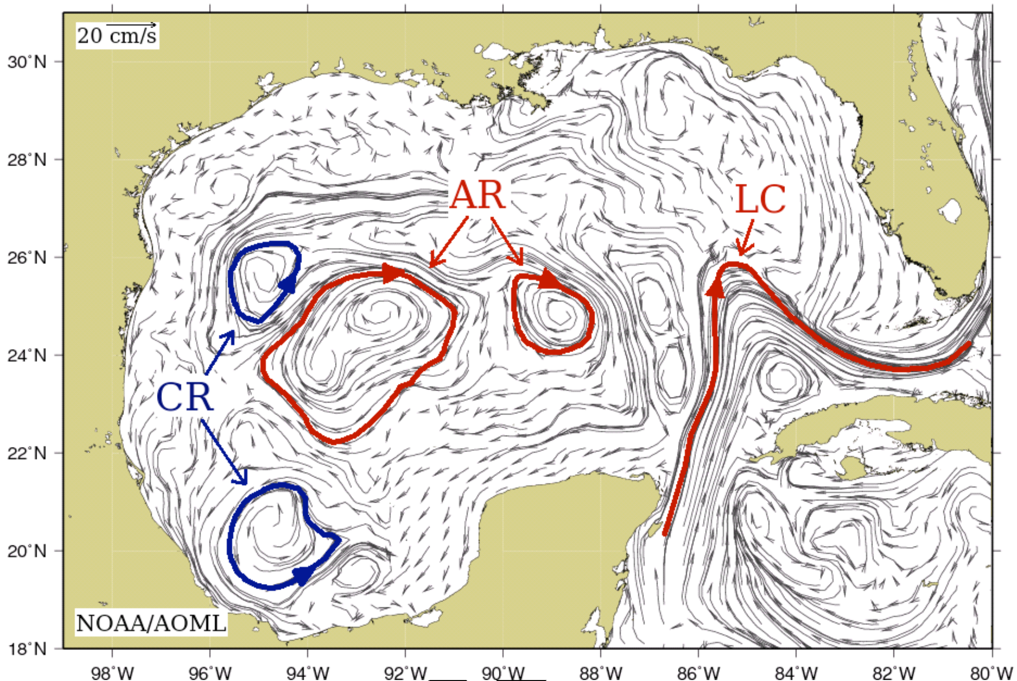

Figure 1. Example of general circulation through the Gulf of Mexico. Gray arrows in the background represent satellite-derived geostrophic currents with red contours highlighting anticyclonic movements (mainly Loop Current, LC, and anticyclonic rings, AR) and blue contours for cyclonic rings (CR). (Courtesy of NOAA/AOML).

The questions of whether and how the dynamics of the GOM have a direct impact on some biological populations are explored herein. Knowledge of the temporal and spatial variability of mesoscale structures in the eastern GOM is fundamental for understanding the environmental conditions that influence distributions of the larvae of different fish species, spawning sites, larval growth and subsequent variability in larval and juvenile survival (Richards *et al.*, 1993). Frontal structures and eddies may influence the spawning strategies of fishes, since they provide necessary feeding resources by concentrating nutrients in certain areas. The influence of mesoscale eddies on larval fish transport and survival depends both on regional oceanographic characteristics, and the strategies of the fish species in question. Feeding and survival conditions have been suggested to be better in eddies (Canino *et al.*, 1991), as high abundances of fish larvae have previously been observed in both anti-cyclonic (Schumacher *et al.*, 1993) and cyclonic (Okazaki *et al.*, 2002) eddies. Larvae retained within eddies have been found to show a lower mortality rate than elsewhere (Bograd *et al.*, 1994). It has also been hypothesized that retention in eddies that move downstream at slower rates than mean currents (Bograd *et al.*, 1994) may enhance delivery of larvae to nursery areas, and may retain them in areas more conducive to survival (Hinckley *et al.*, 2001). Eddies may aid in the retention of fish larvae in coastal areas (Kasai *et al.*, 2002) and may decrease the probability of them being transported offshore into oceanic environments (Bograd *et al.*, 1994). They may also function as a transport mechanism from coastal areas to offshore nursery grounds (Komatsu *et al.*, 2002). In addition, both anticyclonic and cyclonic eddies have been shown to positively affect the abundance and distribution of plankton and fish larvae by entrapment of planktonic organisms (Nakata *et al.*, 2000; Okazaki *et al.*, 2002). Specific influences of eddies on larval fishes depend on several factors, such as the nature of the biological environment that the eddy provides for the larvae in terms of food concentrations and planktonic predators, and the favorability of the environment where larvae are transported by eddies. Moreover, cyclonic eddies may play an important role in primary production through upwelling of nutrient-rich deep water to the euphotic surface layer. This may then cause enhanced zooplankton production, followed by increased ichthyoplankton survival and recruitment (Nakata *et al.*, 2000). For an upwelling event to have any effect on secondary production, the cyclonic eddies would have to endure for several weeks (Fossheim *et al.*, 2005).

Understanding and monitoring the LC and associated ring field becomes critical to the understanding of the distributions of larval fish. Changes in the Yucatan Current (YC) position are correlated with changes in the LC position, suggesting that the separation of LC eddies occurs when cyclonic meanders of the YC move northward and join a semi-permanent meander off the Florida shelf (Molinari and Cochrane, 1972). Although recent studies indicate that Gulf of Mexico and the Caribbean Sea are dynamically inter-dependent (Oey *et al.*, 2005), the manner in which the YC and the LC affect each other with regards to position is not clear. Much of the intrusion variability is associated with the angle at which the current enters the GOM at the

Yucatan Channel (Molinari and Morrison, 1988). Previous analysis of 12 years of data indicated no significant correlation between monthly LC position and Florida Current transport (Maul and Vukovich, 1993). Although the frequencies of ring separation varied, no correlation between ring separation and changes in transport of the Florida Current were found (Sturges, 1992). The annual fluctuations in Loop Current flow were apparently due to wind forcing (Sturges and Evans, 1983).

In summary, when and where mesoscale ocean features occur in the GOM is expected to play an important role in determining a favorable habitat for pelagic species to spawn.

The objectives of this paper are twofold:

i) To gain a deeper understanding of the mesoscale dynamics that are important for larval distribution and transport in the GOM, by means of characterization of their properties, their spatial distribution, and their temporal evolution from 1992 to 2008.

ii) To verify the influence of mesoscale ocean features and sea surface temperature on the distribution patterns of fish larvae spawned in the GOM in the springs from 1993 to 2007, in order to provide a benchmark for future coupled physical and biological studies.

This paper is organized as follows. In section 2 the oceanographic and fisheries data used in this work is described. The methodology used for the analysis of the oceanographic dynamics of mesoscale features in the GOM, and their relation with several larval species is described in section 3. Section 4 contains the results of the analysis and a discussion of their significance. Finally, the conclusions reached in this work are presented in section 5.

2. Data

Throughout all investigations of GOM dynamics conducted since the 1970s, much of the knowledge of ring shedding behavior has been gained using sea surface temperature (SST) fields from satellite infrared (IR) data and a limited number of hydrographic observations. Although IR data continue to be invaluable due to their unsurpassed spatial resolution, they are subject to cloud contamination and temperature limitations during summertime, when the uniformly warm SST does not allow inference of the flow field. On the other hand, altimetry measurements of sea height anomaly (SHA) are not subject to this limitation. Altimetry observations are the main data set of this work, and they are used herein to locate and monitor the LC and associated rings from November 1992 to December 2008.

The fisheries data used in this work consist of absolute values of captured larvae standardized to larval densities (number of larvae per m^3 of sea water filtered). The time period of this data set ranges from April 1993 to June 2007 and belongs to the region in the GOM north of 23°N.

2.1. Oceanographic data

The temporal and spatial resolution of in situ oceanographic observations in the Gulf of Mexico is sparse. However, satellite derived observations of SHA, SST and ocean color offer sufficient temporal and spatial resolution to study the evolution of the main surface mesoscale features and the distribution patterns of larvae spawning in the GOM.

Microwave Optimally Interpolated (OI) SST fields obtained from observations retrieved by the TMI and AMSR-E radiometers onboard the TRMM and Aqua satellites, respectively, are used in this study (http://trmm.gsfc.nasa.gov/ and http://nsidc.org/data/amsre/). These fields have a daily resolution on a 0.25 degree grid. This data set is complemented with gridded fields obtained using SST observations from the Advanced Very High Resolution Radiometer (AVHRR). These fields are available with a resolution of 2 days on an 18 km equal-area grid to complete the period 1993 to 1997 (Ryan et al., 1996). Links between SST values and observations of larvae are determined using these SST fields.

The altimetry data used herein are the optimally interpolated gridded SHA fields according to the methodology of Le Traon *et al.* (1998); with spatial resolution of 0.25 degrees, and temporal resolution of 1 week. The altimetric observations used to produce these gridded fields are obtained from two to four satellites throughout the period of this study.

The main dynamic features in the Gulf of Mexico, including the Loop Current and its intrusion in the Gulf, can be very well observed using high resolution SST observations during the non-summer months of the year when gradients of temperatures in the frontal areas are more intense. Since the goal of the present work includes establishing links between surface ocean features and larvae of several species during the spring months, and sometimes extending the season of study to beginning of summer, altimetry data becomes more appropriate since it can be used to monitor surface ocean features year-round. Therefore, the relationship between ocean dynamics and larval capture data is determined in this work using satellite altimetry. For example, during the month of May 2003, SST, SHA, sea surface height (SSH), and gradient of SSH fields clearly show the LC and a warm ring (Fig 2 a, b, c and d). On the other hand, during the month of June 1998 the LC and a ring cannot be observed with SST (Fig 2e) but are visible using altimetry (Fig 2f, g, h).

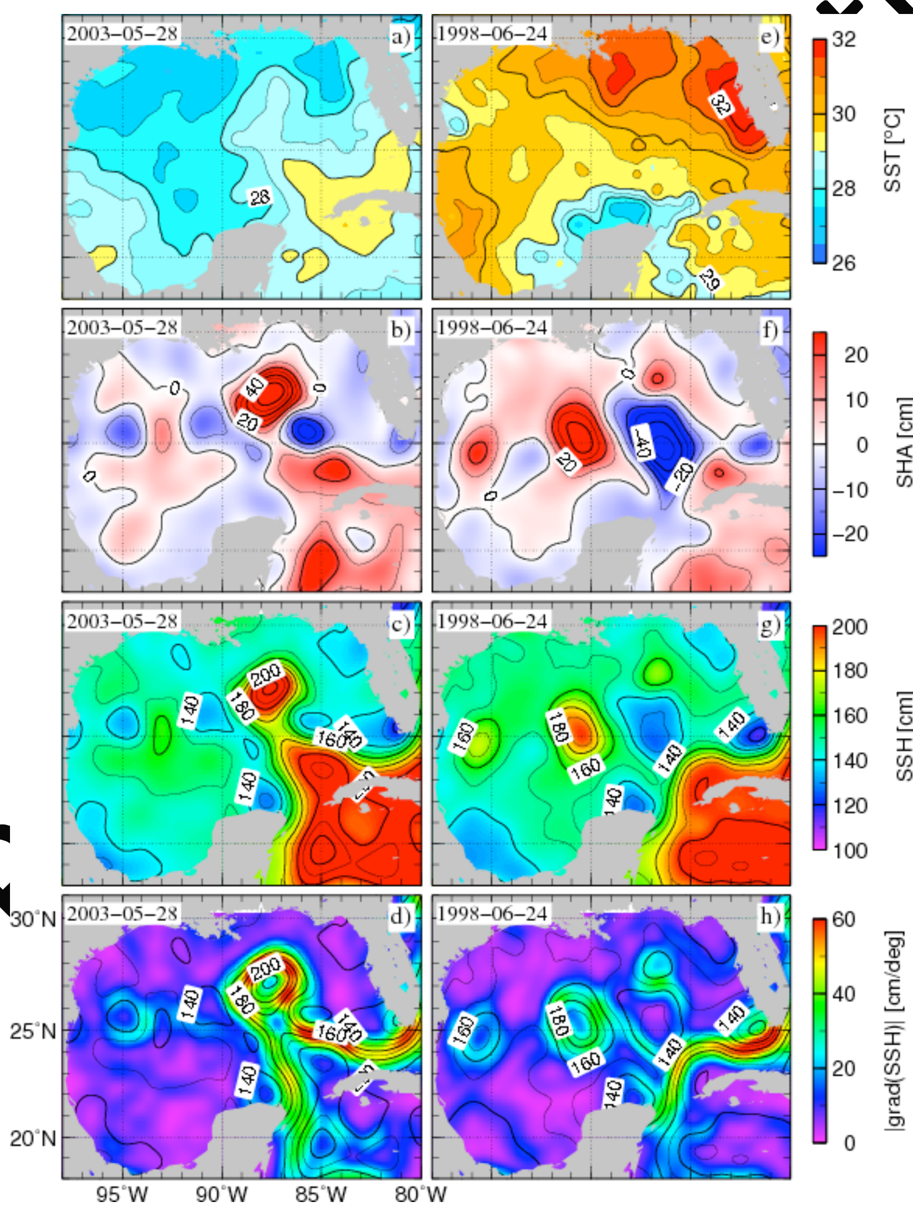

Figure 2. Examples of altimetry fields. Fields on the left illustrate the spring signal of LC northward intrusion in terms of SST (a) SHA (b), SSH (c) and gradient of SSH (d) on May 28, 2003. Fields on the right illustrate the spring signal of a ring separation event in terms of SST (e) SHA (f), SSH (g) and gradient of SSH (h) on June 24, 1998.

In this work, the study of the dynamics of the mesoscale features in the GOM was performed using sea surface height (SSH) fields derived from SHA data. The SSH fields were obtained by adding the altimetry-derived SHA fields to a mean dynamic topography (MDT) of the ocean (Rio and Hernandez, 2004), i.e:

$$SSH = SHA + MDT \quad (1)$$

A few characteristic contours of constant SSH values are used here to define the locations of the LC and cyclonic and anticyclonic rings. Figure 2 c) and g) show the fields of SSH in the GOM in May 28, 2003 and June 24, 1998 where the LC and an anticyclonic ring can be easily observed in red colors, cyclonic rings in blue purple colors and common waters in both images in light blue. Green and dark blue colors also delimit the boundary of anticyclonic and cyclonic features in these fields, respectively.

The geostrophic eddy kinetic energy (EKE) computed from the altimetry fields is $(g^2/2f^2)(\eta_x^2 + \eta_y^2)$, where g is the acceleration of gravity, *f* is the Coriolis parameter, and η_x and η_y are the zonal and meridional SHA gradients, respectively. EKE is used to locate areas of higher velocities, including the jet of the LC.

2.2. Fisheries data

Larval fish data were available for every year from 1993 through 2007 from the National Marine Fisheries Service Southeast Area Monitoring and Assessment Program (SEAMAP) database. Cruises were divided into 2 legs and were conducted throughout the United States Exclusive Economic Zone (EEZ) in the northern GOM only. Figure 3 shows the location of the stations carried out in these surveys. Most of the sampling effort was focused on a one-degree grid of stations, and this grid was usually completed twice in each year, with the exception of 2003 and 2004 when they were completed once. Additional stations were sampled in 1994, 1995, 2005 and 2006. Between 38 and 155 hydrographic-plankton stations were carried out each year, with an average of 94 stations per survey in the 15 years covered by this study. Essentially, at each hydrographic plankton station plankton are collected with bongo and neuston nets, and CTD casts are completed.

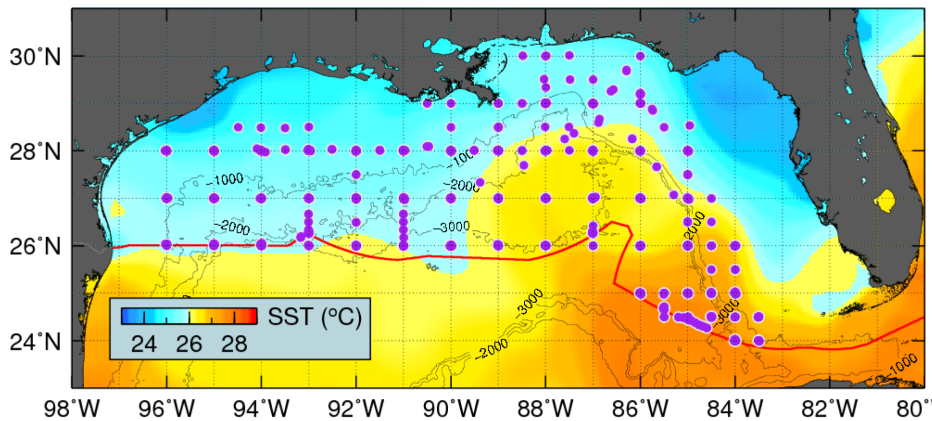

Figure 3. Station locations of the NOAA SEFSC annual larvae survey from 1993 to 2007. The background color is the mean SST for spring 2007. Note that since the locations are repeated every year a single circle may represent several samplings.

Both bongo and neuston net tows are generally completed across the grid of stations in the GOM in late April and May, with sampling continuing into late June in some years. Therefore, analysis of the results presented here corresponds to periods between April and June. Bongo nets are fitted with 333µm mesh, on two 61 cm diameter round frames, and are towed obliquely (Richards *et al.*, 1993), to 200 m depth or to just above the bottom at shallower stations. Nets are towed at 2-3 knots, and sampling takes place during both day and night. Samples from bongo nets are sorted, and larvae identified to the lowest possible taxa at the Polish Plankton Sorting and Identification Center in Szczecin, Poland.

3. Methods

The temporal and spatial variability of the main mesoscale features in the Gulf of Mexico is investigated in terms of the northward and westward intrusion of the LC, the shedding of warm rings, and the characterization of ring shedding events.

3.1. Loop Current spatial variability and local oceanographic features identification

The northward and westward LC penetration is determined from the horizontal gradient of SSH associated with this feature. Specifically, the northernmost and westernmost locations of the SSH maximum gradient contour are used to characterize the shape and position of the LC.

To validate this gradient method, results of present work are compared with other studies for each time step regarding the LC northward penetration and ring separation (Zavala-Hidalgo *et al.*, 2006). A monthly match between rings identified in this work and the results obtained by the previous work is presented in the results section.

A methodology using SSH and grad(SSH) fields is developed in this work to identify the oceanographic features in the GOM. This methodology assigns every grid point in the region to be either a) a region of anticyclonic movement, b) a region of cyclonic movement, c) a boundary of an anticyclonic movement, d) a boundary of a cyclonic movement or e) common GOM waters. According to the convention used here, a location is defined as being in:

a) an anticyclonic region (AR) if $SSH \geq SSH_{max} - n \cdot \sigma(SSH)$

b) a cyclonic region (CR) if $SSH \leq SSH_{min} + p \cdot \sigma(SSH)$

c) an anticyclonic region boundary (AB) if $SSH \geq m \cdot SSH_{max}$ and $grad(SSH) \geq r \cdot \sigma(|SSH|)$

d) a cyclonic region boundary (CB) if $SSH \leq q \cdot SSH_{min}$ and $grad(SSH) \geq r \cdot \sigma(|SSH|)$

e) common waters (CW) if none of the previous conditions is satisfied

where:

$\sigma(SSH)$ is the standard deviation of *SSH* in the region,

$\sigma(|grad(SSH)|)$ is the standard deviation of the absolute value of the gradient of *SSH* in the region.

The five dimensionless parameters m, n, p, q and r are used to calibrate the method. They are determined by tuning the outputs obtained by this method for the summer 2009 with actual satellite-derived SSH fields and geostrophic currents. The values obtained by the tuning for these parameters are:

$m = 0.91 \qquad n = 3.30 \qquad p = 0.60 \qquad q = 1.08 \qquad r = 0.67$

3.2. Loop current ring census and separation events characterization

The size and energy of LC rings depends on latitude, water stratification, bottom topography, and the nature of their generation. These properties can be characterized by undertaking a ring census similarly to those carried out in other regions that used observations of infrared imagery (Brown *et al.*, 1986) or a combination of climatological in situ data and satellite altimetry (Goni *et al.*, 1997; Goni and Johns, 2001).

The LC ring shedding events are detected using estimates of the gradient of sea surface height derived from satellite altimetry observation (Figure 4). A LC ring is considered to be shed on the surface when two conditions are satisfied: a) when the contours of SSH that belong to the higher values of SSH gradient are closed (Figure 4b), and b) when the first condition lasts for a period of time longer than four weeks.

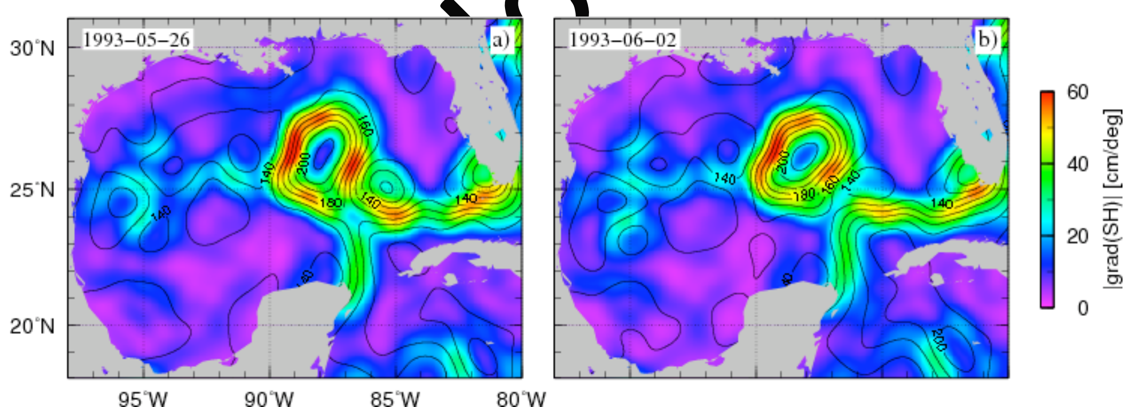

Figure 4. Field of altimetry-derived SSH gradient in the GOM with contours of SSH (in cm, black lines) superimposed.

The life span of a ring is defined as the period of time since the ring is shed until the values of the enclosed dynamic height contours decrease to reach similar values to the surrounding waters.

3.3. Fisheries data analysis

The spring plankton surveys were originally designed to target bluefin tuna larvae. However, larvae of more than 500 taxa have been recorded over the duration of the surveys. In this study, larvae of 6 taxa from three commercially important families are analyzed. In many cases, larvae from closely related species are not distinguishable visually, and so larval groups are merged at the genus, or family, level. Larvae of Coryphaenidae (dolphinfishes hereafter: likely incorporating *Coryphaenia hippurus* and *Coryphaenia equiselis*) are analysed at family level, as are larvae of Lutjanidae (snappers hereafter: likely incorporating up to 19 species from 6 genera: *Apsilus*, *Etelis*, *Lutjanus*, *Ocyurus*, *Pristipomoides* and *Rhomboplites*). Within the family Scombridae (tunas), *Auxis* larvae (likely incorporating larvae of *A. rochei rochei* and *A. thazard thazard*) are analysed at genus level, as are *Thunnus* larvae (likely a mix of *T. albacares* and *T. atlanticus*). Larvae of both *Thunnus thynnus* (bluefin tuna hereafter) and *Euthynnus alleteratus* (little tunny hereafter) are visually distinguishable from other tuna species, and are therefore analyzed at species level.

Larval distribution is related to mesoscale ocean features and their boundaries by carrying out a statistical analysis when catch locations are in anticyclonic locations, anticyclonic boundaries, cyclonic locations, cyclonic boundaries or common waters. These mesoscale features locations are identified using the values of SSH and gradients of sea height as described in the previous section. In addition, larval habitat is characterized here as a function of oceanic-derived variables, such as satellite derived SST and EKE.

4. Results and discussion

4.1. Loop Current northward and westward penetration

Larval fish assemblages of pelagic species are enhanced by the dynamics of the oceanographic system of the LC (Richards *et al.*, 1993). During ichtyoplankton SEAMAP surveys in the spring of 1987, transects made across the LC boundary showed higher displacement volumes of plankton and higher densities of fish larvae (Richards *et al*, 1993). Therefore the LC boundaries, and northern and western excursions of the LC are hypothesized to play a key role in larvae distribution and recruitment.

The northward and westward LC penetration is determined herein by analyzing the 841 weekly fields of SSH gradient in the GOM. Specifically, SSH maximum gradient contours help to objectively characterize the LC position with the northernmost and westernmost locations of the current (fig. 5, for example).

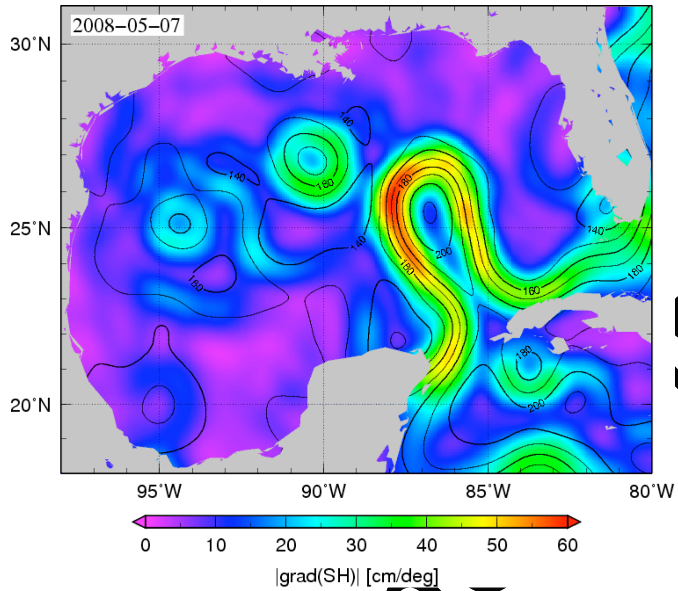

Figure 5. Field of altimetry-derived SH gradient in the GOM on May 7, 2008, with contours of SH (in cm, black lines) superimposed.

Weekly time series of the northernmost position of the LC during the period from November 1992 to December 2008 (Figure 6) are filtered using a Butterworth filter (black line). The filter is designed with order 6 and angular cutoff frequency 1/7 rad/s, which means that the boundary in the filter response is 7 weeks and the maximum filter slope is 20. The vertical blue lines represent the observed ring separation events.

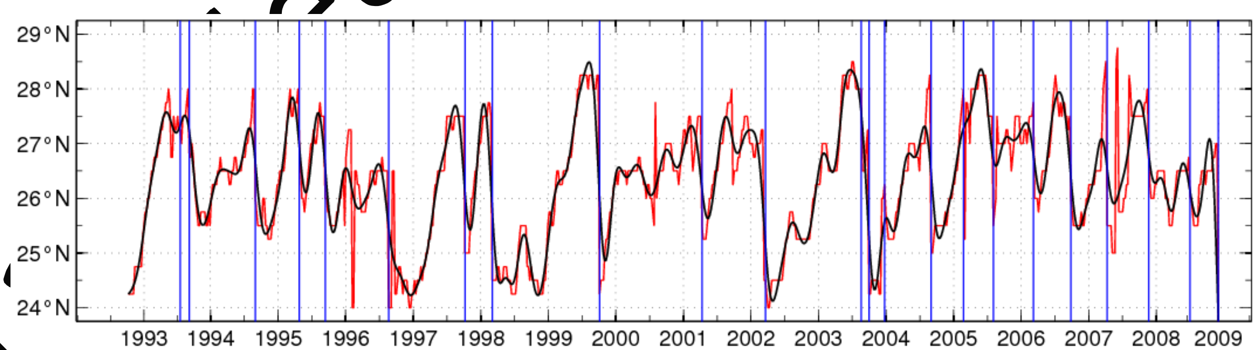

Figure 6. Time series of LC northward penetration, from November 1992 to December 2008. Thick blue lines indicate the time of separation of LC rings.

The northernmost location of the LC varies from 24.25ºN to 28.50ºN, with marked seasonal variations and a mean value of 26.30ºN. The location in summer is significantly more to the north than in the fall season, with winter and spring having values closer to the mean. Previous studies, using data from 47 cruises in the eastern GOM and monthly fields of temperature at 200 m from 1970 to 1976, found that on average the penetration of the Loop Current into the GOM increases during the winter and spring, reaching a maximum in the early summer (Behringer *et al.*, 1977). August appears to be the month with the most occurrences of the northern LC excursions (Figure 7). The separation of the LC rings (thin blue line in figure 6) occurs in 74% of the cases when the northernmost location exceeds 27ºN with separation events happening at a frequency ranging from 2 to 18 months. In general, a north LC location of 27.75ºN leads to a ring separation event after a period of a few weeks to 3 months.

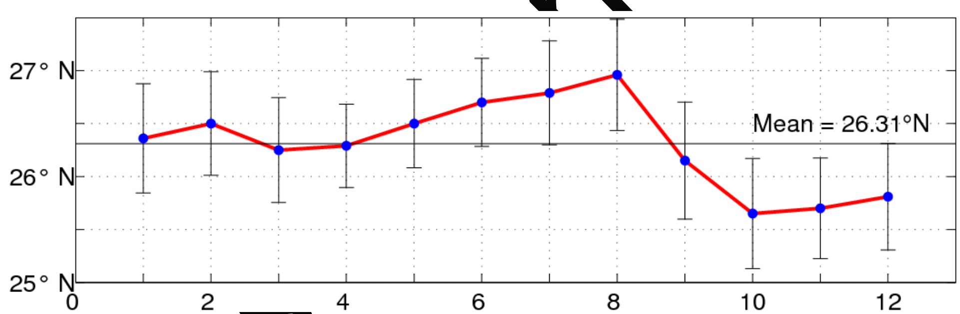

Figure 7. Monthly Mean location of the LC northward penetration. Blue lines indicate standard deviations over the 16 years of data analyzed from January 1993 to December 2008.

The northward penetration of the LC between 1993 and 2008 also exhibits year-to-year variability (Figure 8), showing a maximum in the annual northernmost location of the LC in 2005 and a minimum in the annual northernmost location of the LC in 1998.

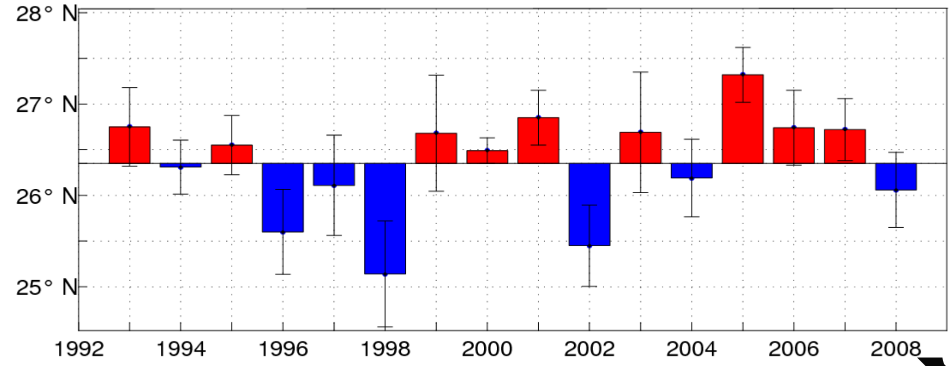

Figure 8. Annual mean location of the LC northward penetration. Blue lines indicate standard deviations over the 16 years of data analyzed, from January 1993 to December 2008.

Weekly time series of the westernmost location of the LC are filtered using a Butterworth filter (black line). The LC westernmost location varies from 91.5ºW to 85ºW, with pronounced variability and a mean value of 87.6ºN. There is a clear year-to-year variability in the westernmost location of the LC, with an annual cycle in the period of time between 1993 and 2005 (Figure 9). When monitoring the time of separation of the LC rings (thin blue line), it is observed that a westernmost location overpassing the 89ºW leads to a ring separation event in 53% of the cases after and a very short period of a few weeks to up to 3 months.

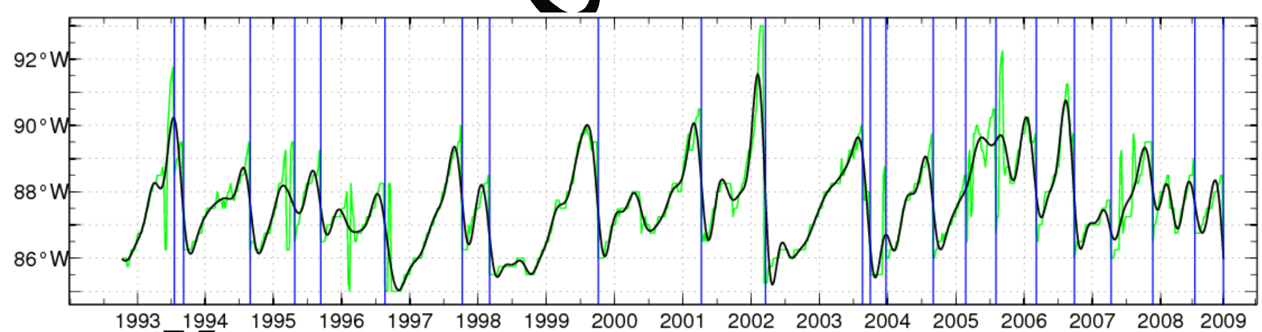

Figure 9. Time series of LC westward penetration, from October 1992 to December 2008. Thick lines indicate the moment of separation of LC rings.

4.2. Ring-separation events

Following the methodology described in 3.2., all the LC ring shedding events are identified between October 1992 and December 2008 (Table I):

Table I. Compilation of ring-separation events. Rings are detected using estimates of the gradient of SSH derived from satellite altimetry observation, from November 1992 to December 2008.

Year	Day	Time between sheddings (months)
1993	Jul 21	
1993	Sep 08	2
1994	Aug 31	11
1995	Apr 26	8
1995	Sep 13	5
1996	Aug 21	11
1997	Oct 08	13
1998	Mar 04	5
1999	Oct 06	18
2001	Apr 11	18
2002	Mar 20	11
2003	Aug 20	17
2003	Oct 01	2
2003	Dec 24	2
2004	Sep 01	9
2005	Feb 23	5
2005	Aug 03	6
2006	Mar 08	7
2006	Sep 27	6
2007	Apr 11	7
2007	Nov 14	7
2008	Jul 02	8
2008	Dec 03	5

A total of 23 rings are identified as shed during the November 1992 to December 2008 study period. Results from January 1993 to August 1999 are compared to results from a previous work on the compilation of ring-separation events (Sturges and Leben, 2000). The present census shows 9 ring separation events between 1993 and 1999, compared with the 10 LC ring detachments reported by the previous work. Excluding a ring shed on April 1996, reported by the previous work but not reported by the present work, there are slight differences in shedding dates between two works.

4.3. Mesoscale structures with significant effects on larval distributions

Associations between larval distributions of bluefin tuna, little tunny, *Thunnus*, *Auxis*, snappers and dolphin-fishes, and mesoscale dynamics in the GOM are presented and discussed in the first part of this section by analyzing observations in larvae distribution over background SSH fields. Then detailed associations between larval catches and the inner and outer regions of mesoscale features are assessed by means of probability bar diagrams. Eventually, further associations between altimetry fields and larval distributions are suggested by relating the number of captures and the proportion of captures to values of SSH.

The spatial distribution and temporal variability of the mesoscale dynamics in the GOM is linked to the distribution patterns of larval spawning (Ortner, 1984; Bakun, 2006). Knowledge of the distribution and variability will enhance our understanding of coupled physical and biological systems. Physical and biological conditions for both larvae and adult fish in the northern GOM exhibit high spatial and temporal variability (Muller-Karger, 1991). Variability in larval abundances has been linked to environmental parameters such as water temperature, salinity, zooplankton abundances, water depth, day length and fluorescence (Muhling *et al.*, 2010; Richardson *et al.*, 2010). Adult fish of the six selected taxa in this work are expected to target specific habitats or oceanographic features where they choose to spawn in order to maximize the survival of their larvae. In addition, fish larvae are capable of detecting and responding to oceanographic gradients (Wilson *et al.*, 2005), and this ability increases with the size of the fish (Kingsford, 2002). When they are newly hatched, larvae drift with the currents; as they grow, however, they have a greater ability to detect where they are in the water column, and to determine their own dispersal through vertical migration/active swimming behavior.

All taxa considered in this study, especially larvae of dolphinfishes and snappers, show patchy distributions with more than 90% of stations showing densities under 0.05 larvae m^{-3} and 82% of stations with even less than 0.02 larvae m^{-3}. Larval abundances vary greatly, with differences of two orders of magnitude between the lowest and highest values. Larval density in positive stations ranged from 0.002 larvae m^{-3} to 0.73 larvae m^{-3}. This patchy distribution may be the result of schooling behaviour of spawners (Smith and Hewitt, 1985) and of sampling methods, which were focused on one-degree grid of stations.

Given the link between temperature and salinity in habitats, the highly energetic scenarios in the GOM, related to the LC and warm ring, are expected to play a key role in determining the abundance and distribution of larvae in the GOM. Analysis of 434 weekly fields between 1993 and 2007 of larval abundance over SSH fields shows definite temporal and spatial relationships between larval distributions and mesoscale structures. These fields indicate that when the LC is in a young state (with northernmost location south of 25.5°N), larvae are more abundant in the eastern Gulf of Mexico than in the central and western part of the basin when the Loop Current is weaker (Figure 10). For instance, 45% of the stations were positive (no zero catches) when surveying the western GOM from May 03 1998 to May 09 1998 (Fig. 10a), while 95% of the stations were positive when surveying the eastern GOM from June 21 1998 to June 27 1998 (Fig. 10b). A similar situation is found during spring 2002: 43% of the stations were positive when surveying the western GOM from April 21 2002 to April 27 2002 (Fig. 10c), while 100% of the stations were positive when surveying the eastern GOM from May 05 2002 to May 11 2002 (Fig. 10d). In both periods, the LC was in a young state and catches in the eastern GOM were found along the northern edges of the LC. Also, larval abundances are often highly spatially autocorrelated: *i.e.*, if one station contained larvae of particular taxa, the neighbouring stations were likely to contain the same taxa as well. This may suggest large-scale spawning when conditions are suitable for a particular taxa (large symbols in Figure 10b).

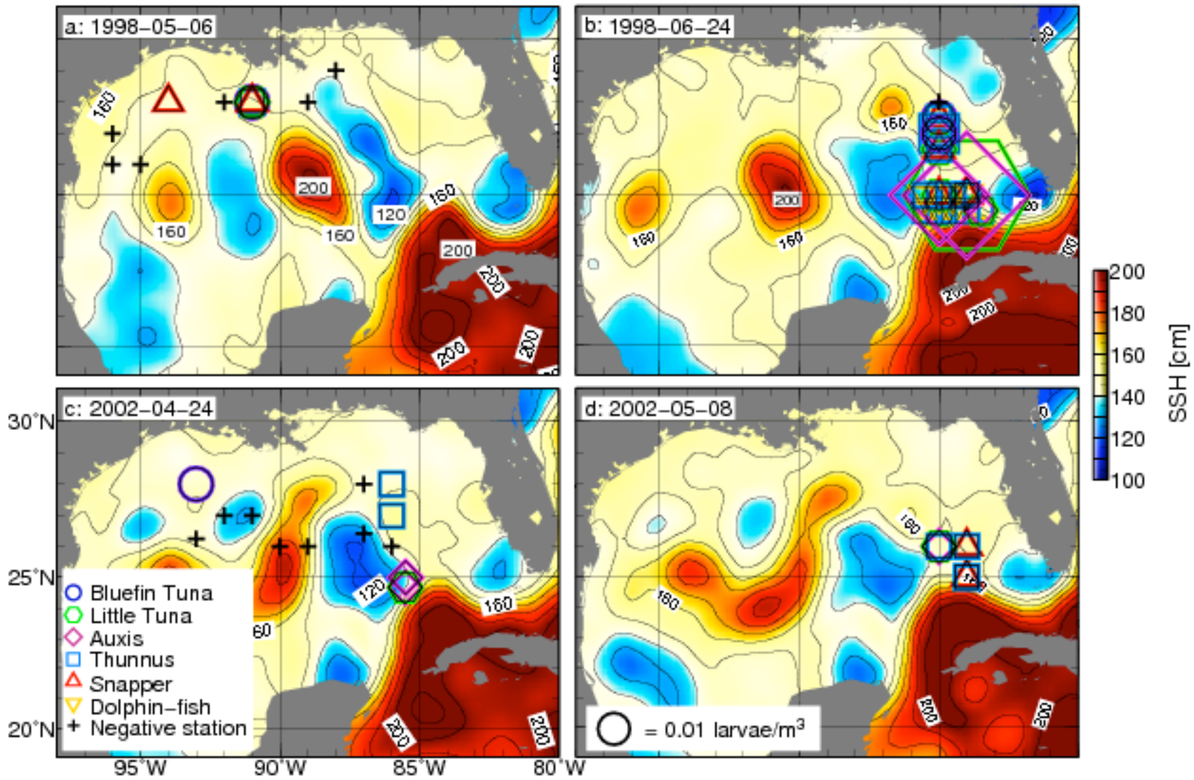

Figure 10. Spatial distribution and density of larvae of bluefin tuna, little tunny, *Thunnus, Auxis*, snappers and dolphin-fishes. Background is SSH field. All fields illustrate an extreme excursion to the south in the northernmost location of the LC in 1998 (a and b) and 2002 (c and d). Fields on the left show larval sampling in the western and central GOM (a and c). Fields on the right show larval sampling in the eastern GOM (b and d).

To further analyze the relationship between LC excursion and larvae distributions, a time series of monthly deviations from the mean northernmost location of LC was analyzed (Fig. 11). Positive vertical bars indicate LC location north of the mean northernmost position, and negative bars indicate LC location south of the mean northernmost position. In order to relate the mesoscale dynamics of the LC to larvae distribution, monthly deviations (anomalies) corresponding to fisheries cruise dates are shaded.

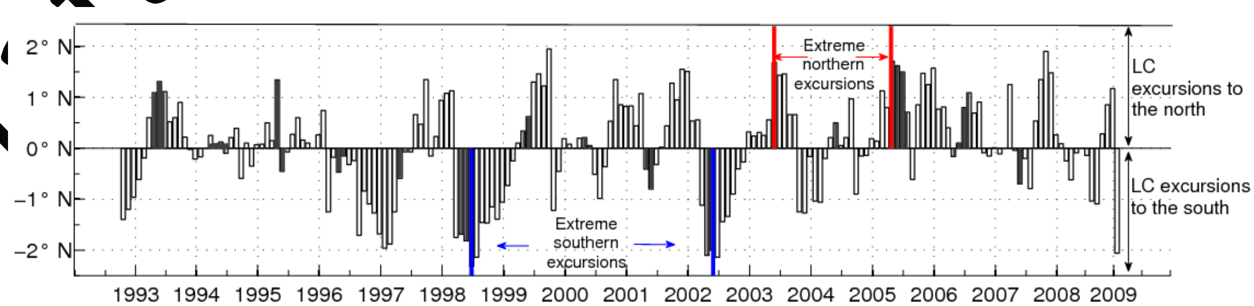

Figure 11. Monthly anomalies of the location of the northward intrusion of the LC. Shaded bars represent monthly anomalies corresponding to fisheries cruise dates. Red and blue lines indicate months of maximum and minimum anomalies observed.

In spring the LC is usually to the north of its mean location (Fig. 7). However, two cases of extreme southern excursions during the spring were found: spring 1998 and spring 2002. In May 1998 and June 1998 there was an extreme excursion to the south of the LC (Fig. 11, blue line), and this southern location (near 25ºN) enhances positive catches between latitudes 25ºN and 28ºN and longitudes 83ºW and 85ºW, just off the LC (Fig. 10b). These are generally areas of poor or zero catches when they are occupied by the LC. In April 2002 and June 2002 there is again a long period of relative minimum position in the LC location (Fig. 11, blue line), and this southern location at 24.5ºN corroborates the previous observation, since the LC in its southernmost location now enhances positive catches between latitudes 24.5ºN and 28ºN and longitudes 83ºW and 86ºW (Fig. 10d).

On the other hand, observations of positive anomalies of the LC northward intrusion suggest that the LC may represent a "desert" within the spawning areas, but this is not a conclusive result since the sampling strategy frequently avoided the warm waters within the LC. Although warm waters may be favorable for egg hatching rates of bluefin tuna (Miyashita *et al*., 2000), and for fast larval growth rates of some species like Atlantic mackerel or northern anchovy (Houde, 1989), retention conditions within the LC are poor because larvae spawned within the LC are advected out of the GOM and northwards along the south eastern United States coast within a period of days (Richards, 1989). In addition, observations suggest that warm-core rings shed by the LC are generally less likely to contain high abundances of larvae. Larvae seem to avoid the core regions of both cyclonic and anticyclonic mesoscale features, and appear to be more abundant at the boundaries and frontal areas (Fig. 12), which is consistent with results obtained using a systematic sampling in the Mediterranean Sea targeting bluefin tuna near frontal areas (Alemany *et al*, 2010). However, observations show that *Thunnus* species are occasionally found within the LC. Similar disparities between abundances of bluefin tuna and other tuna larvae are also found in the Mediterranean (Garcia *et al*., 2005), where high abundances of bluefin larvae have been collected in areas under the influence of anticyclonic gyres.

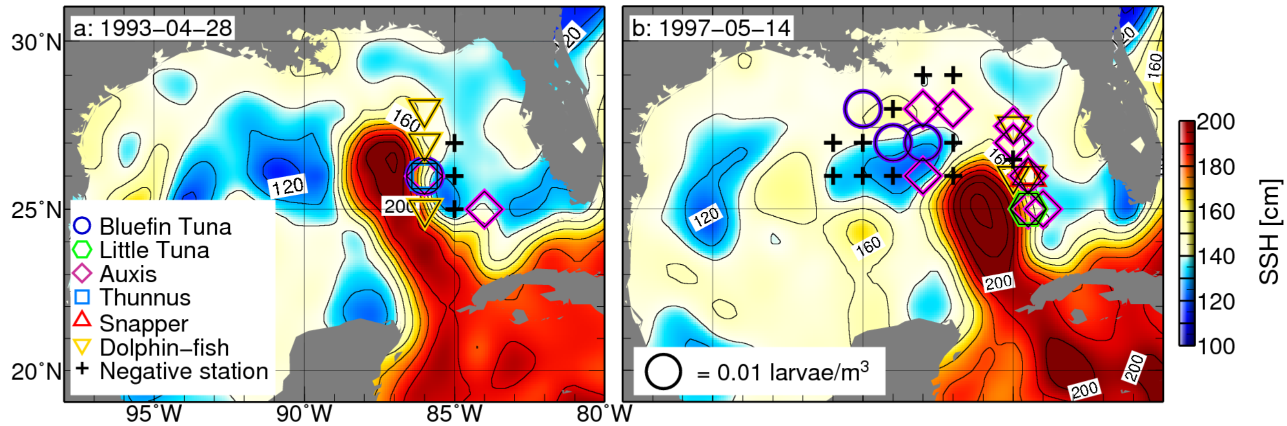

Figure 12. Spatial distribution and density of larvae of bluefin tuna, little tunny, *Thunnus*, *Auxis*, snappers and dolphin-fishes. Background is the SSH field. The field on the left shows catches on frontal areas of the LC on April 28, 1993. The field on the right shows catches on frontal areas of the LC on May 14, 1997.

Although all taxa studied here spawn in a wide range of depths, little tunny and snappers showed a preference for shallower waters, close to the continental shelf. This result is consistent throughout various years of observations and may be due to the usually more productive coastal waters and the scarcity of bigger predators and competitors in these waters (Fig. 13).

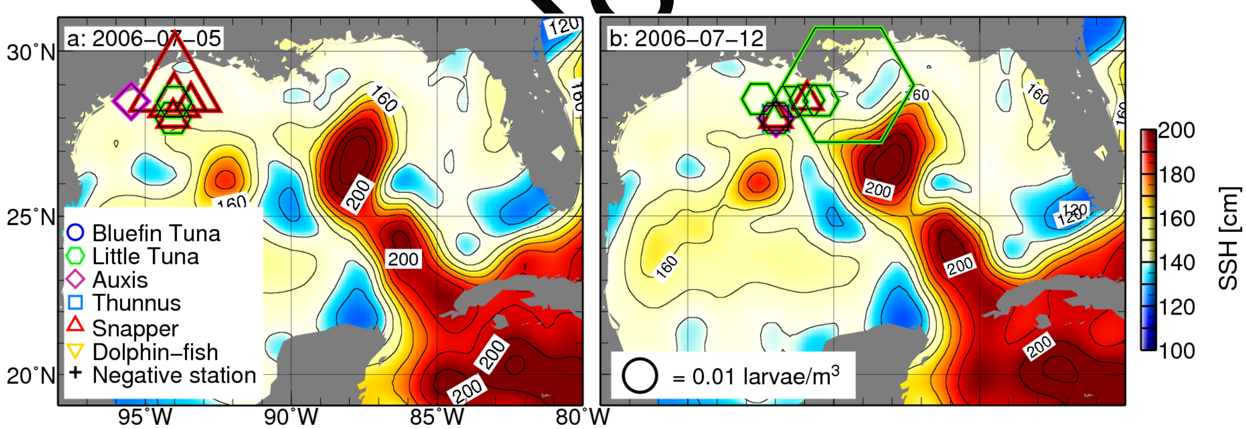

Figure 13. Spatial distribution and density of larvae of bluefin tuna, little tunny, *Thunnus, Auxis*, snappers and dolphin-fishes on July 05 2006 and July 12 2006. Background is the SSH field for previous dates. The field on the left shows an example of the observed preference of snappers for shallower waters. The field on the right shows an example of the observed preference of little tunny for shallower waters.

In order to assess a more detailed association between larval catches and the inner or outer regions of mesoscale features, the capture locations were classified into five different categories: anticyclonic region, anticyclonic boundary, cyclonic region, cyclonic boundary and common waters. This characterization was determined according to the maximum values of SSH, minimum values of SSH, and horizontal gradients of SSH, as explained in section 3.3. From this characterization, bar diagrams are constructed to examine the probability of finding larvae in each of the 5 above-mentioned regions (Table II and Figure 14). The probability of finding larvae of taxon *i* in a oceanic mesoscale feature *j* is calculated herein using the following quotient:

Where c_{ij} is the number of captures of taxon *i* in feature *j*, e_{ij} is the fishing effort when sampling taxon *i* in feature *j*, is the summation of the captures divided by the fishing effort in the five regions, *i* is the taxa (bluefin tuna (1), little tunny (2), *Auxis* (3), *Thunnus* (4), snapper (5), and dolphinfish (6)), and *j* is the region (AR, AB, CR, CB and CW). The fisheries surveys (section 2.2) were conducted in the northern regions of the GOM, which are dominated by oceanic mesoscale features. Since some regions are sampled/surveyed more than others, there is a higher fishing effort in some mesoscale features. Therefore, in the calculation of probabilities, captures of taxon *i* are standardized by dividing by the effort, defined as the total number of times the feature was sampled (with capture or without capture). Although sampling strategies used in the surveys may not be the most adequate, they still provide sufficient information to assess links between larval catches and inner and outer regions of mesoscale features.

Results shown in Table II and Figure 14 define larval distributions of two species (bluefin tuna and little tunny), two genus (*Auxis* and *Thunnus)* and two families (snapper and dolphinfish) in the inner and outer regions of oceanic mesoscale features and provide some insight into the effects of mesoscale structures on larval recruitment in the GOM.

Table II. Captures (c), efforts (e) and probabilities (P) of finding larvae in anticyclonic regions (AR), anticyclonic boundaries (AB), cyclonic regions (CR), cyclonic boundaries (CB) and common waters (CW) for bluefin tuna, little tunny, *Auxis*, *Thunnus*, snappers and dolphinfishes. Calculated from altimetry derived fields and spring sampling from 1993 to 2007.

			AR	AB	CR	CB	CW
Species	Bluefin Tuna	c	31	209	29	60	313
		e	74	76	41	68	117
		P	0.060	0.370	0.095	0.119	0.356
	Little Tunny	c	24	125	3	9	349
		e	62	69	24	48	174
		P	0.086	0.401	0.028	0.041	0.444
Genus	*Auxis*	c	78	350	33	115	1134
		e	81	116	30	74	316
		P	0.094	0.295	0.108	0.152	0.351
	Thunnus	c	301	447	66	175	812
		e	155	170	46	101	339
		P	0.191	0.259	0.142	0.171	0.236
Family	Snapper	c	17	88	2	15	417
		e	66	70	23	52	223
		P	0.068	0.334	0.023	0.079	0.497
	Dolphinfish	c	24	43	9	17	74
		e	77	75	27	57	139
		P	0.167	0.309	0.179	0.161	0.182

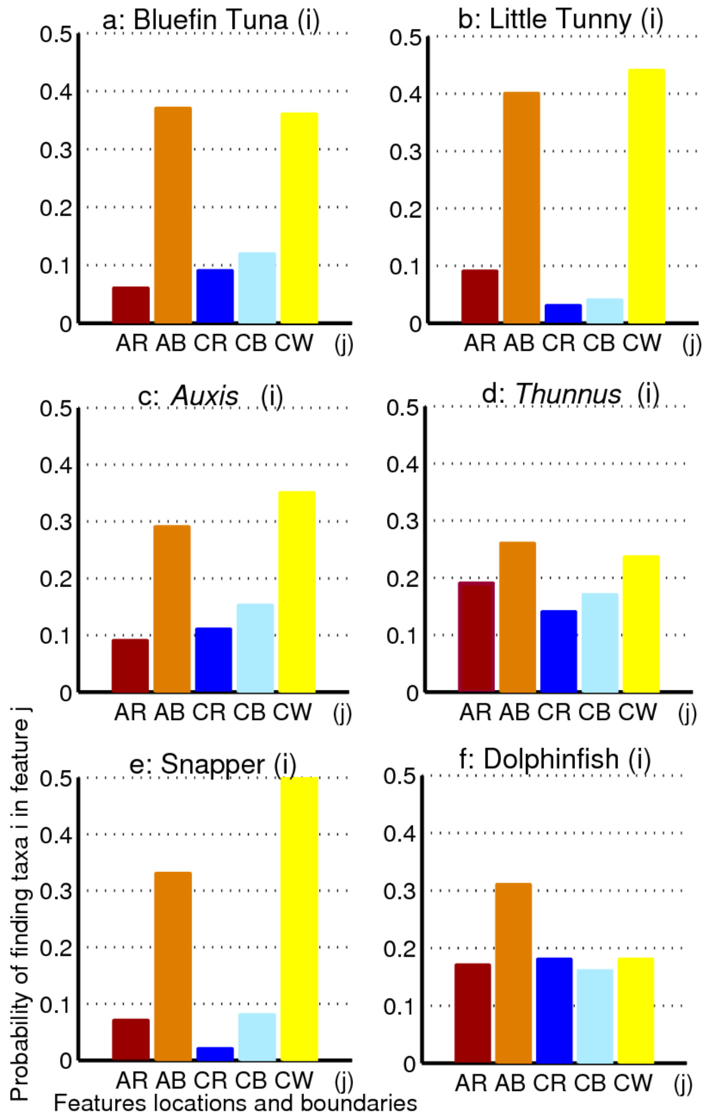

Figure 14. Probability of finding larvae of bluefin tuna (a), little tunny (b), *Auxis* (c), *Thunnus* (d), snappers (e) and dolphinfishes (f) in anticyclonic regions (AR), anticyclonic boundaries (AB), cyclonic regions (CR), cyclonic boundaries (CB) and common waters (CW). Calculated from altimetry derived fields and spring sampling from 1993 to 2007.

The highest distribution of bluefin tuna, little tunny, *Auxis* and snapper is located in the boundaries of anticyclonic features and in common waters. This pattern is more evident in the larval distribution of species (as shown in Figures 14a and b) than in larval distribution of groups that were merged at the genus level (Figure 14c). Results for bluefin tuna, with a probability of 0.37 to be caught in anticyclonic boundaries, is in agreement with previous results found in the western Mediterranean, in which tuna spawning grounds were related to anticyclonic features

(Platonenko and de la Serna, 1997). For little tunny, for example, a probability of 0.44 is expected for catches in regions of common waters and the probability of finding them either in regions of common waters or in anticyclonic boundaries is 0.84. Bluefin tuna, little tunny, *Auxis*, and snapper larvae show a higher distribution in boundaries of anticyclonic features than in core regions of anticyclonic features, and they also show a higher distribution in boundaries of cyclonic features than core regions of cyclonic features. It is hypothesized that larvae may be more common in mesoscale feature boundaries because: 1) they are concentrated by oceanographic processes, 2) feeding conditions are more favorable in convergence zones, which can concentrate planktonic fish larvae, and so larval survival is higher, and 3) adult fishes detect frontal features where they are able to spawn.

Thunnus species, which include larvae of yellowfin tuna and blackfin tuna, were frequently found within anticyclonic and cyclonic region locations (Fig. 14d). This result confirms previous reports showing that adult yellowfin tuna have broader habitat preferences in the GOM in comparison to bluefin tuna (Teo and Block, 2010), and higher tolerances for very warm features, such as the LC and warm LC rings. Although the dolphinfish abundance dataset is scarce and patchy, its larval distribution shows a slightly higher preference for anticyclonic boundaries (P=0.31) and a slightly lower preference for anticyclonic region, cyclonic boundaries, cyclonic regions and common waters (Fig. 14f). Investigation of the abundance in the areas between cyclonic boundaries and anticyclonic boundaries, defined in this work as common waters, indicates that there is a high larval distribution for bluefin tuna, little tunny, *Auxis*, and snapper taxa more likely in between boundary areas.

Once the probabilities of finding larvae in the inner and outer regions of mesoscale features have been analyzed, further associations between altimetry fields and larval distribution are suggested by relating the number and the proportion of captures to values of sea level using satellite-derived SSH fields from 1993 to 2007. For each taxa studied here, Figure 15 shows the mean larval density of the captures (expressed in larvae/m^3) at each SSH and the proportion of captures that are found at each SSH. SSH values are binned to 10 cm intervals. High values of both mean larval density of captures and proportion of captures indicates the SSH at which larvae are more abundant. In order to relate this result to captures in the inner and outer regions of mesoscale features, colored blocks (Fig. 15) represent the SSH domains of cyclonic regions (CR), cyclonic boundaries (CB), common waters (CW), anticyclonic boundaries (AB) and anticyclonic regions (AR), calculated from the mean and standard deviation of the SSH field for each of the 5 regions. These values are detailed in Table III.

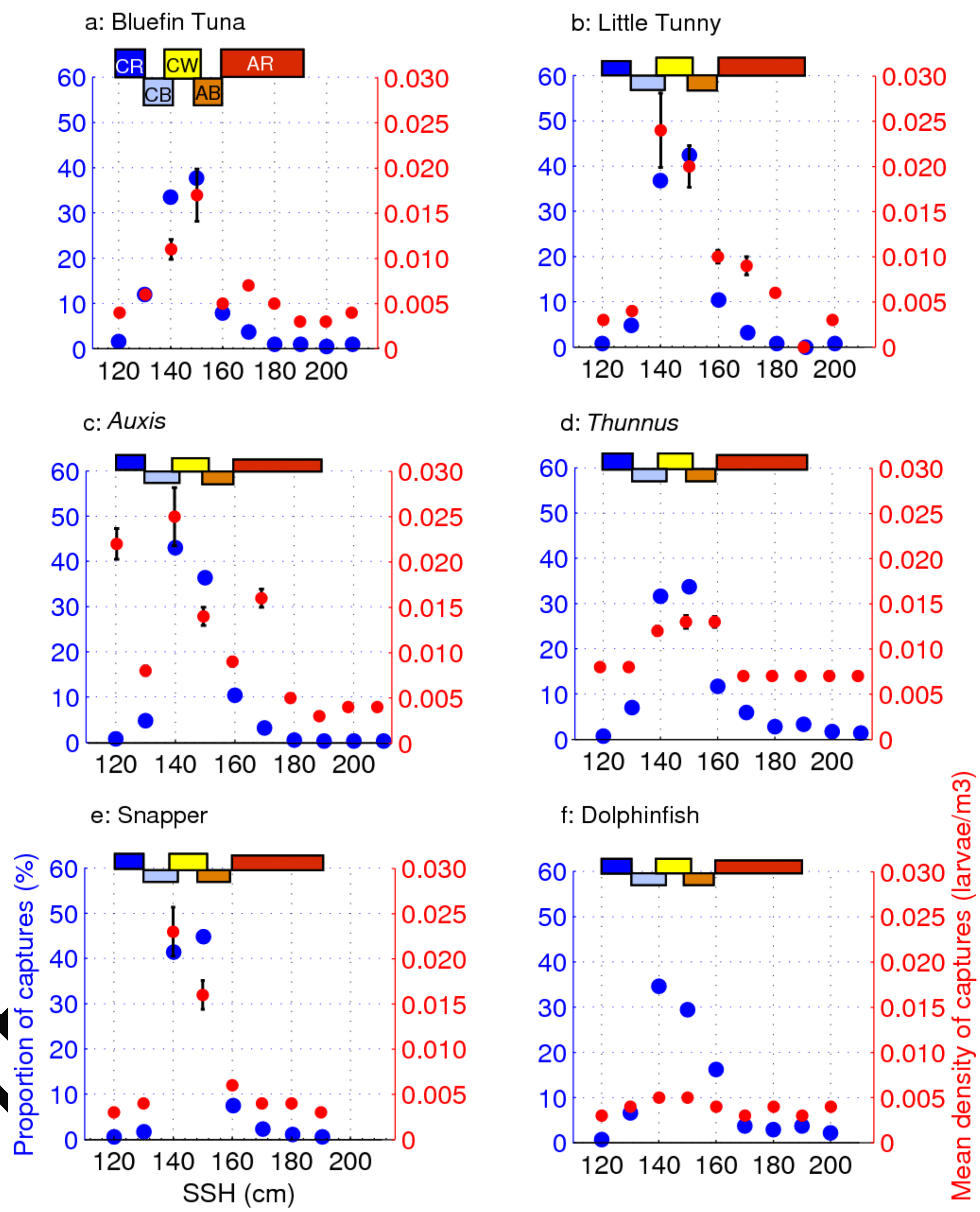

Figure 15. Mean larval density of captures (red circles) and proportion of positive stations (blue circles) for larvae of (a) bluefin tuna, (b) little tunny, (c) *Auxis*, (d) *Thunnus*, (e) snappers, and (f) dolphinfishes in relation to satellite derived observations of sea surface height (SSH), from 1993 to 2007. SSH values are binned to 10 cm intervals.

Error bars represent one standard error. Colored blocks represent SSH intervals of cyclonic regions (CR, dark blue), cyclonic boundaries (CB, light blue), common waters (CW, yellow), anticyclonic boundaries (AB, orange) and anticyclonic regions (AR, red), calculated from the mean and standard deviation of the SSH field for each of the 5 regions.

Table III. SSH minimum, maximum, mean and standard deviation of cyclonic regions (CR), cyclonic boundaries (CB), common waters (CW), anticyclonic boundaries (AB) and anticyclonic regions (AR), calculated from the mean and standard deviation of the SSH field for each of the five regions, from 1993 to 2007

	min (cm)	**max (cm)**	**mean (cm)**	**stdv (cm)**
CR	114	135	124	4.9
CB	121	147	137	5.2
CW	128	161	145	5.1
AB	138	175	153	5.3
AR	153	216	177	15.0

At certain values of SSH, some taxa show high mean density of larvae with a low proportion of captures (*i.e.* Figure 15c at SSH=150 cm), while others exhibit a high proportion of captures with a low mean density (*i.e.* Figure 15f at SSH=140 cm). However, the most interesting features here are SSH values at which both the mean density of larvae and the proportion of captures are high (Figure 15 a, b, c, d, and e, at SSH between 140 cm and 150 cm). Larvae of bluefin tuna, little tunny, *Auxis*, *Thunnus*, snappers, and dolphinfishes show both a high mean larval density and a high proportion of positive stations at SSH of 140 cm to 150 cm, suggesting that they are more abundant in this range of SSH values. This clear preference for moderated levels of SSH is in agreement with larval distributions more likely in common water regions and boundary areas (Fig. 14). Results also show that bluefin tuna, little tunny, *Auxis*, snappers and dolphinfishes are less abundant at extreme values of SSH. *Thunnus* species are more abundant at higher SSH than other species considered here. For example, at high levels of SSH, *Thunnus* larvae show mean densities of 0.008 larvae/m^3 while other larvae exhibit mean densities lower than 0.005 larvae/m^3. This is likely due to higher tolerances for warm waters of the tropical tuna species covered by *Thunnus*. Since SSH is proportional to the integrated vertical temperatures, it indicates that some species are more inclined to be found in specific temperature conditions.

Results and analysis from this section can be used to help in the location of larvae according to different ocean features observed in the field, in particular the probability of finding larvae in the inner and outer regions of mesoscale features in the GOM (Fig. 14) and the predicted abundance of larvae at different SSH (Fig. 15).

5. Conclusions

Satellite altimetry fields were used to identify mesoscale features in the GOM during the period 1993-2007. Larvae data from fisheries surveys collected during this same period were used to identify links between mesoscale features and larval distributions.

The key result obtained in this work is that larvae of bluefin tuna, little tunny, *Auxis* and snapper are preferentially located within the boundaries of anticyclonic features and in GOM common waters. For example, for bluefin tuna, little tunny, and snapper, probabilities above 0.7 are expected for catches in anticyclonic boundaries and common waters (Fig. 14 a, b and e). In addition, for snapper and little tunny probabilities of finding them in cyclonic regions are almost negligible (Fig. 14 b and e).

The results also indicate that high values of proportion of captures and mean density of captures are found between 140-150 cm of SSH. Since SSH is proportional to integrated vertical temperatures, this indicates that most of the taxa studied have a preference for specific temperature conditions.

Although fisheries observations were conducted only during spring months from 1993 to 2007, the oceanographic observations and methodology used in this work allow us to automatically monitor the surface ocean features all year round, due to the incorporation of satellite altimetry data. As a result, times series obtained in sections 4.1 and 4.2 illustrate the spatial and temporal variability of the LC and the temporal variability of the rings shed by the LC, and section 4.3 suggests that the distribution of some larvae are higher within the boundaries of anticyclonic features and in common waters. These results may allow us to hypothesize that captures may also have a similar temporal and spatial variability as features do. For example, the LC location in summer is more to the north than in other seasons, and August appears to be the month with the most occurrences of the northern LC excursion (Fig. 7). This could be translated to a lower probability of capturing certain species in the areas occupied in summer by the LC and a higher probability of capturing certain species in the boundaries of a likely more elongated LC in summer months. Starting in 2003, the LC is more to the north (Fig. 11), and this may also be translated to a lower probability of capturing certain species in the areas occupied by the LC and a higher probability of capturing certain species within the boundaries of the LC. Extreme southern excursions of the LC may also have an impact on larvae distribution. For instance, during extreme southern excursions of the LC (Figs. 10 and 11), high larval distributions are located in the areas that were initially occupied by the LC, particularly along the northern edges of a LC in a young state (with a northernmost location south of 25.5ºN).

The observations also indicate that larvae generally tend to avoid core regions of both cyclonic and anticyclonic mesoscale features, and appear to be more abundant along their boundaries and frontal areas (Fig. 12). It is hypothesized that larvae may be more common in mesoscale feature boundaries because: 1) they are concentrated by oceanographic processes; 2) feeding conditions are more favorable in convergence zones, which can concentrate planktonic fish larvae, and so larval survival is higher; and 3) adult fishes detect frontal features where they are able to spawn.

Analysis of weekly fields between 1993 and 2007 of larvae abundance superimposed upon SSH fields suggests that larval abundances are often highly spatially autocorrelated: *i.e.*, if one station contained larvae of particular taxa, the neighbouring stations were likely to as well (Figs. 10c and 13). This may suggest large-scale spawning when conditions are suitable for a particular taxa.

Although all taxa studied here spawn in a wide range of depths, the observations indicate that some larvae, generally little tunny and snappers, show a preference for shallower waters close to the continental shelf (Fig. 13). This result is consistent throughout the various years of observations, and may be due to the usually more productive coastal waters and the scarcity of bigger predators and competitors in these waters.

This study shows that, in addition to environmental parameters such as water temperature, salinity, zooplankton abundances, water depth or day length, the position and strength of mesoscale features in the GOM is likely to dictate the area and persistence of habitat favorable for larvae growth and survival and, thus, recruitment to adult populations. Interestingly, anticyclonic boundaries and common water regions are suggested as the regions that are most favorable for larvae. The larvae distributions in common water regions may be investigated in future research by tracing frontal zones from SST and ocean color data to overlay on the SSH altimetry. This would give more detail on the 'closeness' of larvae to the features, and would complement present altimetry results.

REFERENCES

Alemany, F., L. Quintanilla, P. Velez-Belchí, A. García, D. Cortés, J.M. Rodríguez, M.L. Fernández de Puelles, C. González-Pola, and J.L. López-Jurado, 2010. Characterization of the spawning habitat of Atlantic bluefin tuna and related species in the Balearic Sea (western Mediterranean). *Prog. Oceanogr.*, **86**, 21-38.

Bakun, A., 2006. Fronts and eddies as key structures in habitat of marine fish larvae: Opportunity, adaptive response and competitive advantage. *Sci. Mar.*, **70**, 105-122.

Behringer, D.W., R.L. Molinari, and J.F. Festa, 1977. The variability of anticyclonic current patterns in the Gulf of Mexico., *J. Geophys. Res.*, **82(34),** 5469-5476.

Bograd, S.J., P.J. Stabeno, and J.D. Schumacher, 1994. A census of mesoscale eddies in Shelikof Strait, Alaska, during 1989. *J. Geophys. Res.,* **99**, 18243–18254.

Brown, O., P. Cornillon, and S Emmerson, 1986. Gulf stream warm rings: A statistical study of their behaviour. *Deep-Sea Res.,* **97** (C6), 9479-9492.

Canino, M.F., K.M. Bailey, and L.S. Incze, 1991. Temporal and geographic differences in feeding and nutritional condition of walleye Pollock larvae Theragra chalcogramma in Shelikof Strait, Gulf of Alaska. *Mar. Ecol. Prog. Ser*., **79**, 27–35.

Elliott, B.A., 1982. Anticyclonic rings in the Gulf of Mexico. *J. of Phys. Oceanogr.*, **12**, 1292-1309.

Forristal, G. Z., K. J. Schaudt, and C. K. Cooper, 1992. Evolution and kinematics of a Loop Current eddy in the Gulf of Mexico during 1985. *J. Geophys. Res.*, **97**, 2173–2184.

Fossheim, M., M. Zhou, K.S. Tande, O.-P. Pedersen, Y. Zhu, and A. Edvardsen, 2005. Interactions between biological and environmental structures along the coast of northern Norway. *Mar. Ecol. Prog. Series*, **300**, 147–158.

Garcia, A., F. Alemany, P. Velez-Belchi, J.L. Lopez Jurado, D. Cortes, J.M. de la Serna, C. Gonzalez Pola, J.M. Rodriguez, J. Jansa, and T. Ramirez, 2005. Characterization of the bluefin tuna spawning habitat off the Balearic Archipielago in relation to key hydrographic features and associated environmental conditions. *Cont. Shelf. Res.,* **16**, 1201-1207.

Goni, G.J., S.L. Garzoli, A.J. Roubicek, D.B. Olson, and O.B. Brown, 1997. Agulhas ring dynamics from TOPEX/POSEIDON satellite altimeter data. *J. Mar. Res.*, **55(5)**, 861-883.

Goni, G., and W. Johns, 2001. A census of orth Brazil current rings observed from TOPEX/POSEIDON altimetry: 1992-1998. *Geophys. Res. Lett.*, **28,** 1-4.

Hinckley S., A.J. Hermann, K.L. Mier, and B.A. Megrey, 2001. Importance of spawning location and timing to successful transport to nursery areas: a simulation study of Gulf of Alaska walleye pollock. *ICES J. Mar. Sci.*, **58**, 1042-1052.

Houde, E.D., 1989. Comparative growth, mortality and energetic of marine fish larvae: Temperature and implied latitudinal effects. *Fish. Bull.*, **87**, 471-495.

Kasai A., S. Kimura, H. Nakata, and Y. Okazaki, 2002. Entrainment of coastal water into a frontal eddy of the Kuroshio and its biological significance. *J. Mar. Syst.*, **37**, 185-198.

Kingsford, M.J., J.M. Leis, A. Shanks, K.C. Lindeman, S.G. Morgan, and J. Pineda, 2002. Sensory environments, larval abilities and local self-recruitment. *Bull. of Mar. Sci.*, **70**,. 309-340.

Komatsu T., T. Sugimoto, K. Ishida, K. Itaya, P. Mishra, and T. Miura, 2002. Importance of the Shatsky Rise area in the Kuroshio Extension as an offshore nursery ground for Japanese anchovy (*Engraulis japonicus*) and sardine (*Sardinops melanostictus*). *Fish. Oceanogr.*, **11**, 354–360.

Maul, G.A., and F.M. Vukovich, 1993: The relationship between variations in the Gulf of Mexico Loop Current and Straits of Florida volume transport. *J. Phys. Oceanogr.*, **23**, 785-796.

Miyashita, S., T. Yuji, S. Yoshifumi, M. Osamu, H. Nobuhiro, T Kenji,. and M. Toshio, 2000. Embryonic development and effects of water temperature on hatching of the bluefin tuna, *Thunnus thynnus. Suisan Zoshoku*, **48**, 199-207.

Molinari, R.L., and J.D. Cochrane, 1972. The effect of topography on the Yucatan Current. In: *Contributions on the Physical Oceanography of the Gulf of Mexico* (edited by L.R.A. Capurro and J.L. Reid). Gulf Publishing Co., Houston, Texas, 149-155.

Molinari, R.L., 1980. Current variability and its relation to sea-surface topography in the Caribbean Sea and the Gulf of Mexico. *Mar. Geod.*, **3**, 409-436.

Molinari, R.L., and J.D. Mayer, 1982: Current meter observations on the continental slope at two sites in the eastern Gulf of Mexico. *J. Phys. Oceanogr.*, **12**, 1480-1492.

Molinari, R.L, and J. Morrison, 1988. The separation of the Yucatan current from the Campeche Bank and the intrusion of the loop current into the Gulf of Mexico. *J. Geophys. Res.*, **93**, 10645-10654.

Muhling, B., J. Lamkin, and M. Roffer, 2010. Predicting the occurrence of Atlantic bluefin tuna (*Thunnus thynnus*) larvae in the northern Gulf of Mexico: Building a classification model from archival data. *Fish. Oceanogr.*, **19**, 526–539.

Muller-Karger, F.E., J.J. Walsh, R.H. Evans, and M.B. Meyers, 1991. On the seasonal phytoplankton concentration and sea surface temperature cycles of the Gulf of Mexico as determined by satellites. *J. Geophys. Res*., **96**, 12645-1266

Nakata H., S. Kimura, Y. Okazaki, and A. Kasai, 2000. Implications of meso-scale eddies caused by frontal disturbances of the Kuroshio Current for anchovy recruitment. *ICES, J. Mar. Sci.,* **57**, 143-151.

Oey, L.-Y., T. Ezer, and H. J. Lee, 2005. Loop Current, rings and related circulation in the Gulf of Mexico: A review of numerical models and future challenges. In: *Circulation in the Gulf of Mexico: Observations and Models. Geophys. Monogr. Ser.*, **161**, 31-56.

Okazaki Y. H. Nakata, and S. Kimura, 2002. Effects of frontal eddies on the distribution and food availability of anchovy larvae in the Kuroshio Extension. *Mar. Freshwater Res.*, **53**, 403-410.

Ortner P.B., R.L. Ferguson, S.R. Piotrowicz, L. Chesal, G. Berberian, and A.V. Palumbo, 1984. Biological consequences of hydrographic and atmospheric advection within the Gulf Loop Intrusion. *Deep-Sea Res.*, **31**, 1101–1120.

Platonenko, S. and J.M. de La Serna, 1997. Observaciones Oceanográficas y Medioambientales en el Mediterráneo Occidental durante la Época de reproducción del Atún Rojo (*Thunnus thynnus* L. 1758). *Col. Vol. Sci. Pap. ICCAT/Recl. Doc. Sci. Cicta/Colecc. Doc. Cient. Cicaa*, **46**, 496-501.

Richards, W.J., T. Lemming, M.F. McGowan, J.T. Lamkin, and S. Kelley-Fraga, 1989. Distribution of fish larvae in relation to hydrographic features of the Loop Current boundary in the Gulf of Mexico. *Rapp. Reun. Cons. Int. Explor. Mer*, **191**, 169–176.

Richards, W.J., T. Lemming, M.F. McGowan, J.T. Lamkin, and S. Kelley-Fraga, 1993. Larval fish assemblages at the Loop Current boundary in the Gulf of Mexico. *Bull. Mar. Sci.*, **53**, 475-537.

Richardson, D.E., J.K. Llopiz, C.M. Guigand, and R.K. Cowen, 2010. Larval assemblages of large and medium-sized pelagic species in the Straits of Florida. *Prog. Oceanogr.*,. **86**, 8-20.

Ryan, E.H., A.J. Mariano, D.B. Olson, and R.H. Evans, 1996. Global Sea Surface Temperature and Currents, *Eos Trans. AGU*, **77**, 46.

Schumacher J.D., P.J. Stabeno, and S.J. Bograd, 1993. Characteristics of an eddy over a continental shelf: Shelikof Strait, Alaska. *J. Geophys. Res*., **98**, 8395–8404.

Shay, L.K., A.J. Mariano, S.D. Jacob, and E.H. Ryan, 1998. Mean and Near-Inertial Ocean Current Response to Hurricane Gilbert. *J. Phys. Oceanogr.*, **28(5)**, 858-889.

Smith, P.E. and R.P, Hewitt, 1985. Sea survey design and analysis for an egg production method of anchovy biomass assessment. *NOAA Tech. Rep., NMFS*, **26**, 17-26.

Sturges, W., 1992. The spectrum of Loop Current variability from gappy data. *J. Phys. Oceanogr.*, **22**, 1245-1256.

Sturges, W., and J.C. Evans, 1983. On the variability of the Loop Current in the Gulf of Mexico. *J. Mar Res.*, **41**, 639-653.

Sturges, W., J.C. Evans, W. Holland, and S. Welsh, 1993. Separation of warm-core rings in the Gulf of Mexico. *J. Phys. Oceanogr.,* **23**, 250-268.

Sturges, A., and R. Leben, 2000. Frequency of ring separations from the Loop Current in the Gulf of Mexico: A Revised Estimate. *J. Phys. Oceanogr.*, **30**, 1814-1819.

Teo, S.L.H., and B.A Block, 2010. Comparitive influence of ocean conditions on yellowfin and Atlantic bluefin tuna catch from longlines in the Gulf of Mexico. PLOS One, 5, E10756.

Zavala-Hidalgo, J., S. L. Morey, and J. J. O'Brien, 2006. On the Loop Current eddy shedding variability. *Atmósfera,* **19 (1)**, 41-48.